Communication in Physical Sciences, 2023, 10(3):147-155

Removal of Cadmium Ion from Aqueous Solution by oyster-based Based Calcium Oxide Nanoparticles

Attah Chuks Emmanuel

Received:07 May 2023/Accepted 14 December 2023/Published 26 December 2023

Abstract: *Environmental challenges associated with the management of non-biodegradable solid waste are best overcome by three cardinal waste management protocols, which are re-use, recover and recycle. The conversion of oyster shells to calcium oxide nanoparticles using the sol-gel method is reported in this work. The nanoparticles showed a crystal nature with average crystalline sizes of 16.85 and 2.705 nm based on the Scherrer and Williamson Hall equations respectively. The synthesized calcium oxide nanoparticles were characterized with XRD and employed in the removal of cadmium ions from aqueous solution through adsorption. Adsorption efficiency approaching 100% was observed at [Cd^{2+}] at 4 pm, alkaline pH and contact period of 70 min. The adsorption of the dye was spontaneous and accepted the mechanical of physical adsorption. The study confirmed that calcium oxide nanoparticles can completely remove cadmium ions from the solution.*

Keywords*: Solid waste, non-biodegradable, heavy metal resource recovery, remediation*

Attah Chuks Emmanuel
Department of Chemistry
Federal University of Petroleum Resources Effurun,
Delta State, Nigeria
Email: attah.chuks@fupre.edu.ng
Orcid id: 0009-0002-6953-6244

1.0 Introduction

Nanoparticles are known for their outstanding properties, which have aided various applications of these unique materials in different sectors including agriculture, environment, electronics, fire fighting, materials, etc (Eddy *et* al., 2024a-b; Gultekin *et al*., 2024; Larranaga-Tapia *et al*., 2024). The market growth rate for nanoparticles is currently outscoring other forms of materials and there are some indications that if the current trend is not checked, there could be a future challenge in other sectors. One of the major challenges that can be significantly detrimental could be the diversion of other materials for the production of nanoparticles. Fortunately, there is currently growing exploitation of waste materials in the synthesis of nanoparticles such as plant waste, animal shells, animal wastes, industrial wastes, etc Essien *et al*., 2023; Ekwumemgbo *et al.*, 2023; Odiongenyi, 2022; Odiongenyi and Afangide, 2019). Solid wastes generated by agricultural, industrial, domestic and natural activities may have toxic impacts on the disposal environment. However, if these wastes can be recycled, and reused or resources can be recovered from them, then a cleaner environment can be secured to a good extent. One of the major sectors in which nanoparticles have played significant roles is the environmental sector. For example, nanoparticles can be used for adsorption removal of contaminants from the atmosphere, soil and water through adsorption or photocatalyzed degradation. Their large surface area, high porosity, high crystallinity, high ratio of surface area to volume, high thermal stability, resistance to chemical attacks, low band gap and high electrical and mechanical properties (Melhi, 2023).

Cadmium is one of the most toxic heavy metals that have received environmental attention concerning methods for the treatment of cadmium-contaminated environments.

Several advantages have been reported on the adsorption removal of cadmium from aqueous solution using nanoparticles compared to other materials (Madawala *et al*. 2023; Zhou *et al*., 2022). Given the high toxicity of cadmium, the need to withdraw them from the environment, and the advantages that can be gained in recovering resources from oyster wastes for the remediation of Cd^{2+}, the current study is aimed at synthesizing calcium oxide nanoparticles (CaONPs) from oyster wastes and to apply them for the remediation of Cd^{2+} contaminated water.

2.0 Materials and Methods

Oyster shells were taken from a dumpsite in Oron. They were washed dried and crushed to powder. The ground sample was used as a precursor for the production of CaONPs as described by Eddy *et al*. (2023a-b). The produced CaONPs were also employed for bath adsorption removal of different concentrations of Cd^{2+} (1, 2,3 and 4 ppm) under varying conditions such as time and pH. The concentration of Cd^{2+} removed at any instant was determined using an atomic absorption spectrophotometer. The percentage of Cd^{2+} removed was evaluated through the difference between the initial or inlet concentration (C_0) and outlet concentration (C_f) according to the following equation,

$$\frac{C_0 - C_t}{C_0} \times \frac{100}{1} \quad (1)$$

In the batch adsorption study, 100 ml of the solution was used in each case and the equilibrium amount of the metal ion removed was evaluated by replacing the denominator of equation 1 (i.e C_0) with the mass of the adsorbent.

3.0 Results and Discussion

3.1 XRD analysis

Fig. 1 shows the XRD spectrum of the CaONPs synthesized from oyster shells while Table 1 presents parameters deduced from the spectrum. From the displayed XRD pattern, the most prominent peak is found at 2θ = 34.19 ° and corresponds to the Miller indices of 2 0 0. Other peaks were found at {2Theta] positions of 18.07, 47, 29.50, 47.29 and 50.92 ° and are ascribed to CaO with various Miller indices as presented in Table 4.1.

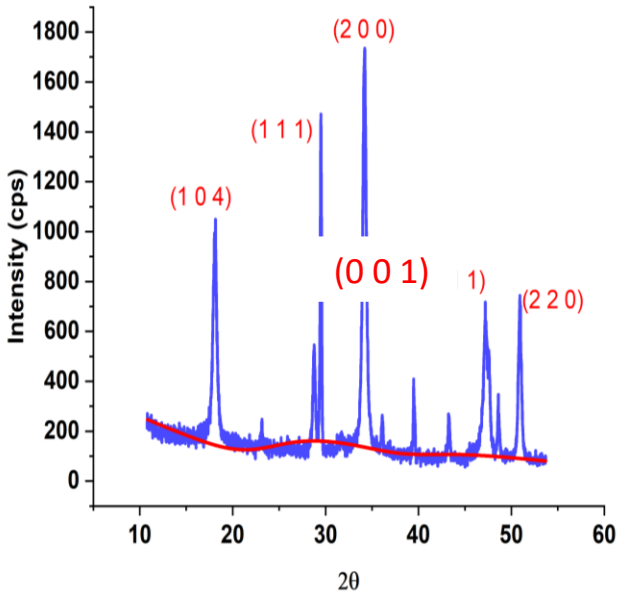

Fig.1: XRD pattern of CaONPs synthesized from oyster shell

The evaluated peaks, especially the principal peak are in good agreement with values reported for CaONPs synthesised from different sources (Eddy *et al*., 2022a, 2023 a-b; Kelle *et al*., 2023; Ogoko *et al*., 2023; Jayaprabakar *et al*., 2023; Nayar *et al*., 2021).

The crystalline size of nanoparticles is a significant parameter related to the dislocation density of a crystal. Equation 2 represents the Scheerer equation, which was used to evaluate the crystalline size of the nanoparticles (Eddy *et al*., 2022b)

$$d_x = \frac{k\lambda}{FWHM * cos\theta} \quad (2)$$

where k and λ represent Scherrer's constant and the X-ray wavelength respectively. Calculated values of the crystalline size for different diffraction angles are also recorded in

Table 1, which shows a range corresponding to 11.82 to 22.20 nm. Consequently, the average crystalline size is 16.85 nm, which confirms that the material is a nanoparticles because the particle size fits into the range of 0 to 100 nm (Khine *et al*., 2022).

Table 1: Crystal parameters for the synthesised

[2Theta]	Area	FWHM	d_x (nm)	δ (nm^{-1})	h	k	l	$d_{(hkl)}$ (nm)	$d_{(\theta)}$ (nm)
18.07	636.77	0.6371	13.19	0.08	0	0	1	0.4991	0.0707
29.50	1249.84	0.4659	18.42	0.05	1	1	1	0.2882	0.1146
34.19	1171.53	0.4659	18.64	0.05	2	0	0	0.2496	0.1323
47.29	707.71	0.7667	11.82	0.08	3	1	1	0.1505	0.1805
50.92	349.53	0.4142	22.20	0.05	2	2	2	0.1441	0.1935

The crystalline size of the nanoparticles was also evaluated using the Willamson Hall equation (equation 3), which related the crystalline size to the diffraction angle and Scherrer parameters as follows (Eddy *et al*., 2023)

$$\beta_{Total} cos\theta = 4\epsilon sin\theta + \frac{k\lambda}{d_x} \qquad (3)$$

where β_{Total} is the total full with at half maximum and ϵ is the macrostrain parameter. The Williamson-Hall plot is shown in Fig. 2. Based on the values obtained for the intercept and slope of the Williamson-Hall plot, the crystalline size and microstrain were calculated as 2.705 nm, and 0. 0433.

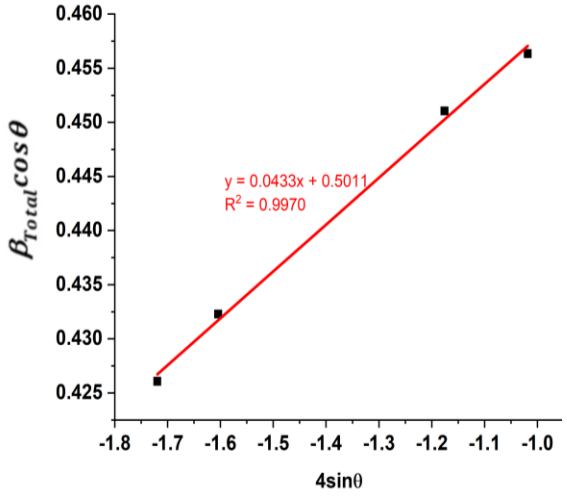

Fig. 2: Williamson Hall plot for the calculation of the crystalline size of the CaONPs

The calculated crystalline size is lower than the value obtained from the Scherrer equation, which may be due to the influence of line broadening and microstrain. The evaluated microstrain is also low and indicates the stability of the crystal to dislocation. The low micro strain value also shows a strong compromise to the dislocation density values (recorded in Table 1) that were obtained as a reciprocal of the crystalline size (i.e $\delta = 1/d_x$), which range from 0.05 to 0.08 nm^{-1} as shown in Table 1.

The Miller indices for the synthesised CaONPs were recorded in Table 1. The lattice parameters for this crystal are $a = b = c =$ 0.4991 nm while the magnitude of the angles are $\alpha = \beta = \gamma = 90°$. The interplanar distance can be evaluated by substituting the listed Bravais parameters into the following equation,

$$\frac{1}{d_{hkl}^2} = \frac{h^2}{a^2} + \frac{k^2}{b^2} + \frac{l^2}{c^2} \qquad (4)$$

However, for this crystal, the lattice parameters are equal. Therefore, equations 5 and 6 are most appropriate

$$\frac{1}{d_{hkl}^2} = \frac{h^2 + k^2 + l^2}{a^2} \qquad (5)$$

$$d_{hkl} = \frac{a}{(h^2 + k^2 + l^2)^{\frac{1}{2}}} \qquad (6)$$

d_{hkl} values evaluated with equation 6 are recorded in Table 1 and indicated the observed range of 0.14 to 0.50 nm. The ditsnce between

place was also calculated using the Bragg diffraction equation, which can be written as,

$$d_\theta = \frac{n\lambda}{2sin\theta} \quad (7)$$

Recorded $d_{(\theta)}$ values (Table 1 shows a range of 0.07 to 0.19 for n values = 1. The two sets of values show a strong negative correlation with R^2 = 0.9742 (Fig. 3)

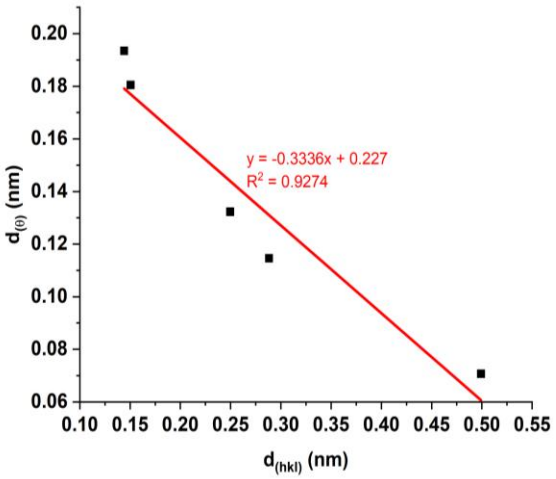

Fig. 3: Correlation plot showing values of interplanar distance in CaONPs crystal, evaluated based on the Miller indices and the diffraction angle

3.2 Adsorption study

The synthesised nanoparticles were applied to remove trace concentrations (1 to 4 ppm) of cadmium ions from aqueous media. Fig. 4 and 5 show the variation of the percentage removal efficiency with concentration at different periods of contact and different pH. From Fig. 4, it is observed that the amount of Cd^{2+} removed at a given time increases with an increase in concentration. This is due to an increase in the number of heavy metal ions diffusing to the surface of the adsorbent as the concentration increases. The increment became more significant because the nanoparticles are known for possessing a large surface area of adsorption and high porosity, which contributes to ensuring that the number of active available sites is significantly large. Therefore, except all the adsorption sites are fully occupied, adsorption will increase with an increase in concentration. The interplay of time with concentration led to the observation that with an increase in time, the adsorption efficiency of the CaONPs increases. This is because time is of the essence considering the diffusion of the molecules to the surface and subsequent adsorption. Therefore, the higher the period of contact, the more the tendency towards adsorption.

Fig. 5 shows that the interplay of pH with concentration also leads to a similar observation, which is at higher pH, adsorption is better. The pH at zero charge of CaONPs is about 6.6 (Eddy *et al*., 2023a). Since Cd^{2+} is a divalent positive ion, it would be preferentially adsorbed better at pH greater than 6.6 (i.e; alkaline pH) than in acidic pH is revealed by the plots (Fig. 5 and Fig. 6). The pattern of variation of adsorption with time (Fig.7) also matched the explanation that justifies why adsorption increases with an increase in the period of contact.

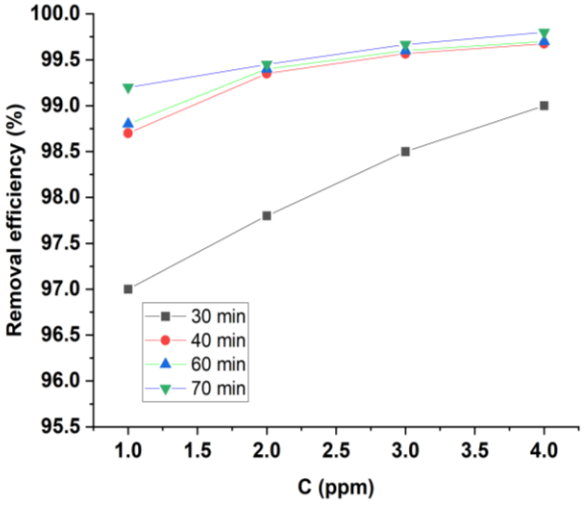

Fig. 4: Variation of the concentration of Cd^{2+} removed by CaONP with concentration for different contact time

3.3 Adsorption isotherm

The tests for the bested-fitted isotherm that can describe the adsorption characteristics of CaONPs for Cd^{2+} showed that the Freundlich isotherm is best preferred based on the R^2 values obtained

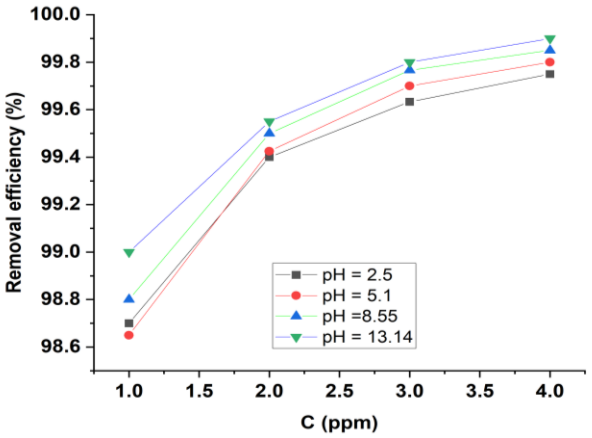

Fig. 5: Variation of the concentration of Cd^{2+} removed by CaONP with concentration for different pH

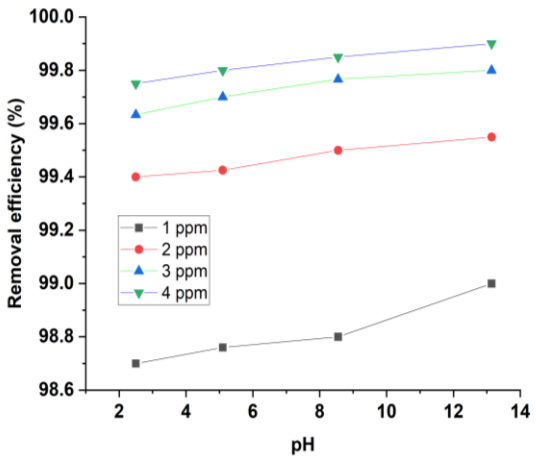

Fig. 6: Variation of the concentration of Cd^{2+} removed by CaONP with pH for different concentration of crystal violet dye

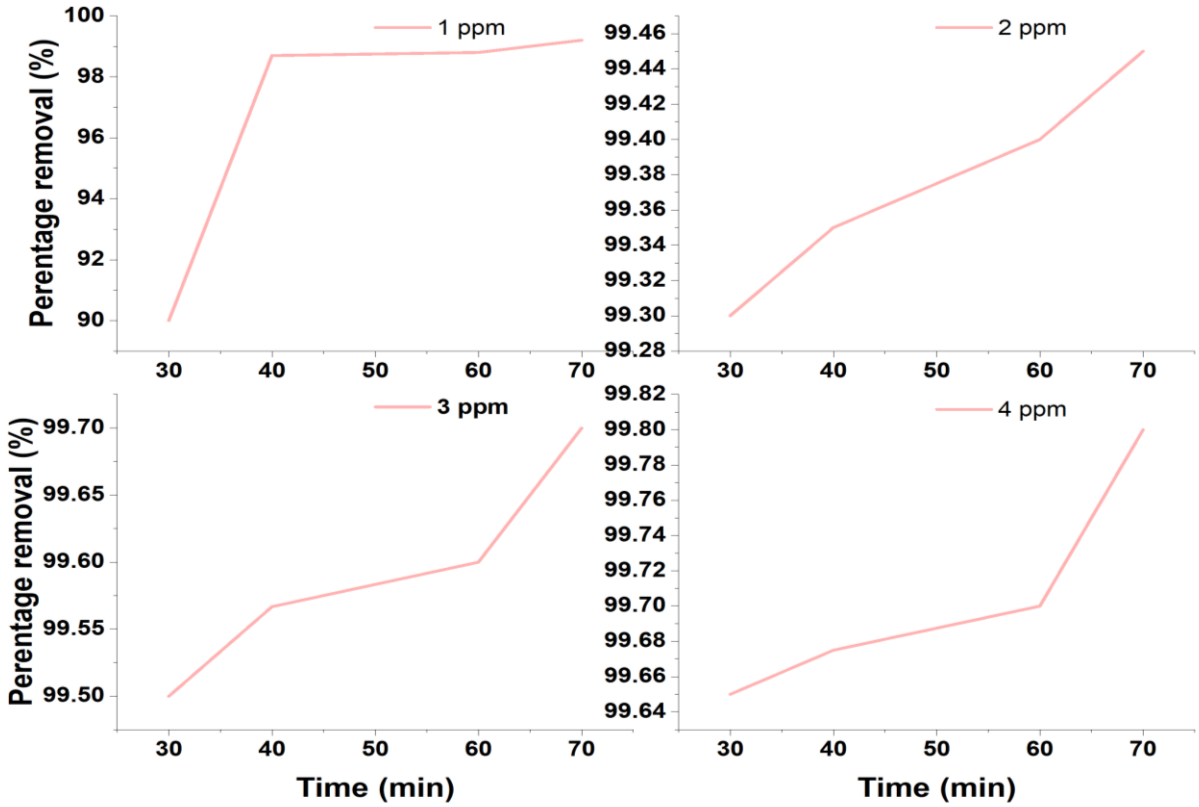

Fig. 7. Variation of the concentration of Cd^{2+} removed by CaONP with time

The Freundlich equation can be written as follows,

$$lnQ_e = lnK_F + \frac{1}{n} lnC_e \quad (8)$$

In the above equation, K_F is the Freundlich constant while n is the adsorption intensity parameter. In Fig. 8, the Freundlich isotherm is shown but parameters calculated from the plots at various experimental time intervals are presented in Table 2. The model reveals that the intensity of adsorption decreases with the period of contact. Generally, values of 1/n

lower than unity signify favourable adsorption. The lower the value, the better the adsorption. Therefore, the information deduced from the Freundlich plots confirms that the adsorption of Cd^{2+} by CaONPs is favourable while the intensity of the adsorption increases with an increase in time.

The Freundlich adsorption constant was also used to evaluate the value of the free energy of adsorption based on equation 9 (Odoemelam and Eddy, 2008),

$$\Delta G^0_{ads} = lnQ_e + \frac{1}{n} lnC_e \qquad (9)$$

Calculated values of the standard free energy of adsorption (Table 2) showed a range of 76.23 to -76.51 J/mol while the average value is 76.42 J/mol. Since these values are negatively less than -40 kJ/mol (which defines the threshold for chemical adsorption mechanism), the adsorption of Cd^{2+} on CaONPs is spontaneous and is consistent with the mechanism of physical adsorption.

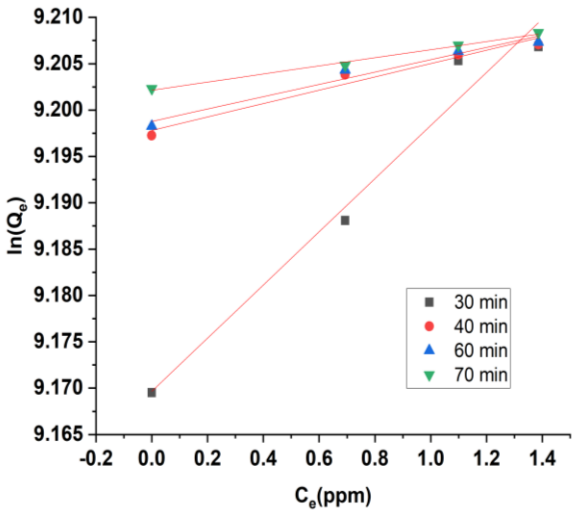

Fig. 8: Freundlich plot for the adsorption removal of Cd^{2+} by CaONPs after various periods of contact

Table: Parameters for the adsorption of Cd^{2+} by CaONPs according to the Freundlich model

Time (min)	1/n	R^2	lnk_{ads}	ΔG^0_{ads} $(\frac{J}{mol})$
30	0.0287	0.9716	9.1697	-76.2369
40	0.0072	0.9669	9.1978	-76.4705
60	0.0066	0.9667	9.1987	-76.478
70	0.0044	0.9919	9.2021	-76.5063

4.0 Conclusion

The study shows that CaONPs have been successfully synthesised from oyster shells. The synthesized product displayed crystalline properties that are in line with literature values. They showed a strong affinity for the adsorption of Cd^{2+} from aqueous solution. The adsorption efficiency increases with time, concentration and pH. Based on the results obtained from the study, CaONPs is a good adsorbent for the removal of Cd^{2+} from aqueous solution.

5.0 Acknowledgement

The author acknowledges the National Research Fund of the Tertiary Education Trust Fund of Nigeria for sponsoring this research through the Principal Investigator, Prof. Nnabuk Okon Eddy (Grant number: TRTF/ES/DR&D-CE/NRF2020/SETI/98/VOL.1) of the University of Nigeria, Nsukka.

6.0 References

Eddy, N. O., Edet, U. E., Oladele J. O., Kelle, H. I., Ogoko. E. C., Odiongenyi, A. O., Ameh, P., Ukpe, R. A., Ogbodo, R., Garg, R. and Garg, R. (2023c). Synthesis and application of novel microporous framework of nanocomposite from trona for photocatalysed degradation of methyl orange dye. *Environmental Monitoring and*

Assessment. doi : 10.1007/s10661-023-12014-x

Eddy, N. O., Garg, R., Garg, R., Aikoye, A. & Ita, B. I. (2022b). Waste to resource recovery: mesoporous adsorbent from orange peel for the removal of trypan blue dye from aqueous solution. *Biomass Conversion and Biorefinery*, DOI: 10.1007/s13399-022-02571-5.

Eddy, N. O., Garg, R., Garg, R., Eze, S. I., Ogoko, E. C., Kelle, H. I., Ukpe, R. A., Ogbodo, R. & Chijoke, F. (2023a). Sol-gel synthesis, computational chemistry, and applications of CaO nanoparticles for the remediation of methyl orange contaminated water. *Advances in Nano Research*, https://doi.org/10.12989/anr.2023.15.1.000

Eddy, N. O., Garg, R., Garg, R., Garg, R., Ukpe, R. A. & Abugu, H. (2024a). Adsorption and photodegradation of organic contaminants by silver nanoparticles: isotherms, kinetics, and computational analysis. *Environ Monit Assess*, 196, 65, https://doi.org/10.1007/s10661-023-12194-6.

Eddy, N. O., Odiongenyi, A. O., Garg, R., Ukpe, R. A., Garg, R., El Nemir, A., Ngwu, C. M. & Okop, I. J. (2023b). Quantum and experimental investigation of the application of *Crassostrea gasar* (mangrove oyster) shell–based CaO nanoparticles as adsorbent and photocatalyst for the removal of procaine penicillin from aqueous solution. *Environmental Science and Pollution Research*, doi:10.1007/s11356-023-26868-8.

Eddy, N. O., Ukpe, R. A., Ameh, P., Ogbodo, R., Garg, R. & Garg, R. (2022a). Theoretical and experimental studies on photocatalytic removal of methylene blue (MetB) from aqueous solution using oyster shell synthesized CaO nanoparticles (CaONP-O). *Environmental Science and Pollution Research*, https://doi.org/10.1007/s11356-022-22747-w.

Eddy, N. O., Ukpe, R. A., Garg, R., Garg, R., Odionenyi A. O., Ameh, P. & Akpet, I, N. (2024b). Enhancing Water Purification Efficiency through Adsorption and Photocatalysis: Models, Application and Challenges. *International Journal of Environmental Analytical Chemistry*, doi: 10.1080/03067319.2023.2295934.

Ekwumemgbo, P. A., Shallangwa, G. A. & Okon, I. E. (2023). green synthesis and characterization of iron oxide nanoparticles using Prosopis Africana leaf extract. *Communication in Physical Science*, 9, 2, pp. 125-136.

Essien, U. I., Odiongenyi, A. O., Obadimu, C. O. & Enengedi, I. S. (2023). Investigation of Snail shells as an Adsorbent and Precursor for the synthesis of Calcium Oxide Nanoparticles for the Removal of Amoxicillin from Aqueous Solution. *Communication in Physical Science*, 9, 4, pp. 453-464.

Gultekin, H.. E., Yasayan, G., Bal-Ozturk, A., Bigham, A., Simchi, A., Zarepour, A., Iravani, S. & Zarrabi, A. Advancements and applications of upconversion nanoparticles in wound dressings. *Mater. Horiz*. doi :10.1039/D3MH01330H

Jayaprabakar, J., Karthikeyan, A., Anand, K. V., Arunkumar, T., Anbazhaghan, N. & Rangasamy, G. (2023). Synthesis and characterization of calcium oxide nano particles obtained from biowaste and its combustion characteristics in a biodiesel-operated compression ignition engine. *Fuel*, 350, https://doi.org/10.1016/j.fuel.2023.128839 .

Kelle, H. I., Ogoko, E. C., Akintola O & Eddy, N. O. (2023). Quantum and experimental studies on the adsorption efficiency of oyster shell–based CaO nanoparticles (CaONPO) towards the removal of methylene blue dye (MBD) from aqueous

solution. *Journal: Biomass Conversion and Biorefinery*, DOI : 10.1007/s13399-023-04947-7.

Khine, E.E., Koncz-Horvath, D., Kristaly, F., Ferenczi, T., Karacs, G., Baumli, P. & Kaptay, G. (2022). Synthesis and characterization of calcium oxide nanoparticles for CO_2 capture. *J Nanopart Res* 24, 139 (2022). https://doi.org/10.1007/s11051-022-05518-z.

Larranaga-Tapia, M., Betancourt-Tower, B., Videa, M., Antunes-Ricardo, M. & Cholula-Diaz, J. I. (2024). Green synthesis trends and potential applications of bimetallic nanoparticles towards the sustainable development goals 2030. *Nanoscale Adv.*,6, pp. 51-71. https://doi.org/10.1039/D3NA00761H.

Madawala, C. K., Jahinge, T. H. L., Rathnayake, K. T. & Perera, B. A. (2023) Adsorption of cadmium (II) from aqueous solutions by coconut dregs residue: Kinetic and thermodynamic studies, *Separation Science and Technology*, 58:11, 1972-1984, DOI: 10.1080/01496395.2023.2227914.

Melhi, S. (2023) Recyclable magnetic nanocomposites for efficient removal of cadmium ions from water: performance, mechanism and isotherm studies, *Environmental Pollutants and Bioavailability*, 35, 1, doi: 10.1080/26395940.2022.2163922.

Nayar, P., Waghmare, S., Nageshwar, P., Najar, M., Singh, U. & Agnihotri, A. (2021). Preparation of calcium oxide nanoparticles from industry rejects: Recovery and value addition of mineral values. *Materials Today: Proceedings*, 39, 4, pp. 1722-1726, https://doi.org/10.1016/j.matpr.2020.06.300.

Odiongenyi, A. O. & Afangide, N. U. (2019). Adsorption and thermodynamic studies on the removal of congo red dye from aqueous solution by alumina and nano-alumina. *Communication in Physical Science*, 4, 1, pp. 1-7.

Odiongenyi, A. O. (2022). Influence of Sol Gel Conversion on the Adsorption Capacity of Crab Shell for the Removal of Crystal Violet from Aqueous Solution. *Communication in Physical Science*, 8, 1, pp. 121-127.

Odoemelam, S. A. & Eddy, N. O. (2008). Effect of pyridoxal hydrochloride-2, 4-dinitrophenyl hydrazone on the corrosion of mild steel in HCl. *Journal of Surface Science and Technology* 24, 1, 2, pp. 1-14.

Ogoko, E. C., Kelle, H. I., Akintola, O. & Eddy, N. O. (2023). Experimental and theoretical investigation of *Crassostrea* gigas (gigas) shells based CaO nanoparticles as a photocatalyst for the degradation of bromocresol green dye (BCGD) in an aqueous solution. *Biomass Conversion and Biorefinery*. https://doi.org/10.1007/s13399-023-03742-8

Zhou, Z., Dong, Y., Zhu, L., Xia, X., Li, S., Wang, G. & Shi, K. (2022). Effective and stable adsorptive removal of cadmium(II) and lead(II) using selenium nanoparticles modified by microbial SmtA metallothionein. *Chemosphere*, 307, 2, https://doi.org/10.1016/j.chemosphere.2022.135818.

Compliance with Ethical Standards Declarations

The authors declare that they have no conflict of interest.

Data availability

All data used in this study will be readily available to the public.

Consent for publication

Not Applicable

Availability of data and materials

The publisher has the right to make the data public.

Competing interests

The authors declared no conflict of interest.

Funding

The work is fully sponsored by the Tertially Education Trust Fund under the National Research Fund (Grant number: TRTF/ES/DR&D-CE/NRF2020/SETI/98/VOL.1) through Prof. Nnabuk Okon Eddy as the Principal Investigator

Authors' contribution

All the components of the work were carried out by the author